Bioorganic & Medicinal Chemistry Letters 20 (2010) 3618–3622

Contents lists available at ScienceDirect

Bioorganic & Medicinal Chemistry Letters

journal homepage: www.elsevier.com/locate/bmcl

Design of 1-piperazinyl-4-arylphthalazines as potent Smoothened antagonists

Brian S. Lucas [a,*], Wade Aaron [b], Songzhu An [b], Richard J. Austin [b], Matthew Brown [a], Hon Chan [c], Angela Chong [b], Randall Hungate [a], Tom Huang [c], Ben Jiang [c], Michael G. Johnson [a], Jacob A. Kaizerman [a], Gary Lee [b], Dustin L. McMinn [a], Jessica Orf [b], Jay P. Powers [a,†], Minqing Rong [b], Maria M. Toteva [d], Craig Uyeda [c], Dineli Wickramasinghe [b], Guifen Xu [c], Qiuping Ye [c], Wendy Zhong [b]

[a] Department of Medicinal Chemistry, AMGEN, 1120 Veterans Blvd., S. San Francisco, CA 94080, USA
[b] Department of Oncology, AMGEN, 1120 Veterans Blvd., S. San Francisco, CA 94080, USA
[c] Department of Pharmacokinetics and Drug Metabolism, AMGEN, 1120 Veterans Blvd., S. San Francisco, CA 94080, USA
[d] Department of Small Molecule Process and Product Development, AMGEN, 1120 Veterans Blvd., S. San Francisco, CA 94080, USA

ARTICLE INFO

Article history:
Received 9 March 2010
Revised 22 April 2010
Accepted 26 April 2010
Available online 28 April 2010

Keywords:
Smoothened
SMO
Smo
Hedgehog
Hh
Patched
Ptch
Cancer
Medulloblastoma

ABSTRACT

The Hedgehog (Hh) signaling pathway regulates cell proliferation and differentiation in developing tissues, and abnormal activation of the Hh pathway has been linked to several tumor subsets. As a transducer of Hh signaling, the GPCR-like protein Smoothened (Smo) is a promising target for disruption of unregulated Hh signaling. A series of 1-amino-4-arylphthalazines was developed as potent and orally bioavailable inhibitors of Smo. A representative compound from this class demonstrated significant tumor volume reduction in a mouse medulloblastoma model.

The Hedgehog (Hh) signaling pathway plays a significant role in the regulation of cell growth and differentiation during embryonic development.[1] Abnormal activation of the Hh pathway has been implicated in a number of cancer[2,3] types, including basal cell carcinoma[4] and medulloblastoma.[5] Members of the Hh family (Sonic Hedgehog, Indian Hedgehog, and Desert Hedgehog) can bind to the 12-pass transmembrane protein Patched (Ptch), a repressor of Smo signaling. Thus, the Hh family of proteins indirectly activate Smo, often measured downstream as a corresponding increase in Gli transcription factors. Interruption of Hedgehog signaling via Smo antagonism was first established with plant alkaloids including cyclopamine,[6] and has subsequently resulted in considerable interest in targeting Smo for cancer.[7]

Our investigation[8] began with a high-throughput screen which identified a number of potent Smo antagonists, including the phthalazine **1** (Fig. 1). The Smo antagonism (IC_{50}) of 22.0 and 7.0 nM in our respective mouse (mSmo)[9] and human (hSmo)[10] assays was confirmed upon resynthesis. Lead compound **1** was further evaluated in a number of high-throughput assays, including stability to microsomes[11] and inhibition of CYP enzymes 3A4 and 2D6.[12] Compound **1** was found to have relatively high turnover in rat (RLM) and human (HLM) microsomes, as well as high levels of CYP 2D6 inhibition. Therefore, we initiated a medicinal chemistry program around **1** with the aim of maintaining potency for

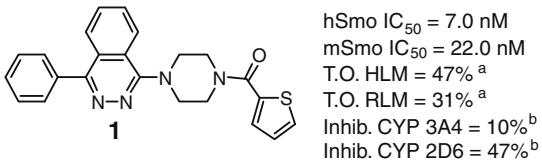

Figure 1. Lead compound **1**. [a]Percent of **1** turned over (consumed) after 30 min incubation with human (HLM) or rat (RLM) liver microsomes.[11] [b]Percent inhibition of CYP 3A4 or 2D6 at 3 μM concentration.[12]

* Corresponding author. Tel.: +1 650 244 2128.
E-mail address: blucas@amgen.com (B.S. Lucas).
† Current address: ChemoCentryx, Inc., 850 Maude Avenue, Mountain View, CA 94043, USA.

0960-894X/$ - see front matter © 2010 Elsevier Ltd. All rights reserved.
doi:10.1016/j.bmcl.2010.04.110

Table 1
Smoothened antagonism and microsomal stability of amide modifications

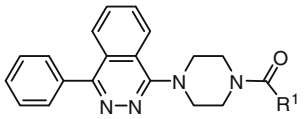

Compound	R^1	hSMO IC_{50}[a] (nM)	T.O. HLM[b] (%)	T.O. RLM[b] (%)	CYP 3A4 inhib.[c]	CYP 2D6 inhib.[c]
1	2-Thienyl	7.0	48	31	<10	47
2	2-Furyl	13.0	43	32	<10	48
3	2-Thiazoyl	9.5	48	25	<10	89
4	Methyl	91.0	10	10	<10	29
5	Phenyl	19.0	19	12	<10	11

[a] Values are the mean of a minimum of two measurements with a standard deviation of 35% of the mean.
[b] Percent turnover after 30 min incubation with human (HLM) or rat (RLM) liver microsomes.
[c] Percent inhibition of CYP 3A4 or 2D6 at 3 μM concentration.

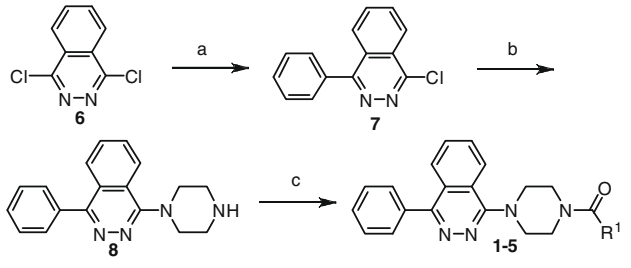

Scheme 1. Synthesis of unsubstituted piperazine compounds **1**–**5**. Reagents and conditions: (a) PhBr, *n*-BuLi, $ZnCl_2$, $Pd(PPh_3)_4$, −78 °C to rt, 48%; (b) piperazine, MIBK, reflux, 100%; (c) R^1COCl, Et_3N, 30–54%.

Smo, improving metabolic stability, and reducing P450 inhibition, beginning with the replacement of the thiophene ring in **1** (Table 1).

Synthesis of compounds **1**–**5**[13] was accomplished according to Scheme 1. Dichlorophthalazine **6** was subjected to Negishi cross-coupling conditions[14] to afford phenylpthalazine **7**. Treatment of **7** with piperazine in refluxing methylisobutyl ketone (MIBK)[15] afforded intermediate **8**. Compounds **1**–**5** were obtained by acylation of **8** with an appropriate acid chloride.

While heterocyclic thiophene replacements such as furyl (**2**) and thiazoyl (**3**) did not address microsomal turnover, the simple bioisosteric phenyl group in compound **5** afforded reasonable potency, reduced turnover in microsomes, and minimal CYP 3A4 and 2D6 inhibition. Thus, the benzoyl piperazine motif was incorporated in subsequent compounds as shown in Scheme 2. Starting once again from 1,4-dichlorophthalazine **6**, piperazines **9** and **10** were incorporated to afford piperazinylphthalazines **11** and **12**, respectively. Key intermediates **11** and **12** were subjected to a combination of deprotection with trifluoroacetic acid (TFA, **11** only), acylation with benzoyl chloride, and a palladium catalyzed cross-coupling in various order to generate compounds **13**–**43**.

Metabolite ID studies of **5** performed in rat and human hepatocytes identified the piperazine ring as an additional site for metabolism (Fig. 2).[16] Investigation of methylation about the piperazine ring revealed significant effects on potency and stability as described in Table 2. The 2-*S*-methyl piperazine **13** afforded a nearly fourfold increase in potency as well as lowered turnover in human microsomes. Incorporation of the regioisomeric 3-*R*-methyl piperazine (**16**) led to even more potent Smo antagonism, however microsomal clearance was increased significantly over the other piperazine cores.

Our initial SAR around the pendant aryl group was performed on the unsubstituted piperazine core. A simple Topliss[17] scan (Table 3, **5** and **17**–**20**) showed insufficient spread in potency and thus failed to provide clear direction. Additional analogs (**21**–**25**) were synthesized but likewise showed little dynamic range in terms of potency. However, the relative microsomal stability and general

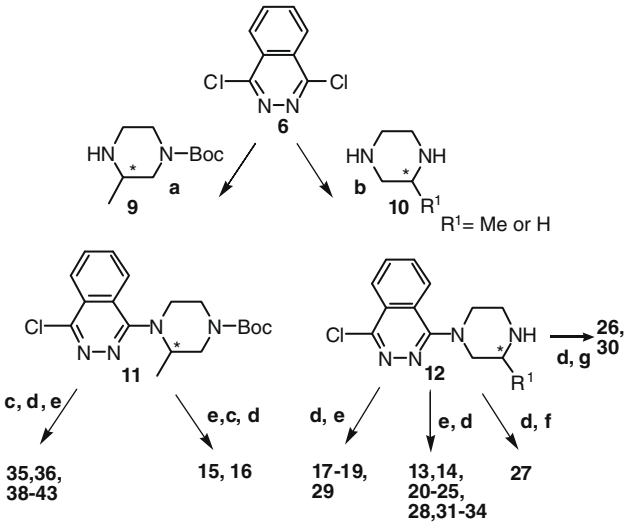

Scheme 2. Synthesis of benzoyl-piperazine bearing compounds **13**–**43**. (a) Neat, 120 °C, 27–50%; (b) MIBK, reflux, 71–89%; (c) TFA, DCM, 100%; (d) Benzoyl chloride, Et_3N, DCM, room temperature, 35–89%; (e) Ar–$B(OH)_2$,, $Pd(PPh_3)_4$, Na_2CO_3, toluene/water, reflux, 23–95%; (f) 3-pyridylboronic acid, K_3PO_4, $Pd_2(dba)_3$, SPhos 87%; (g) Aryl-$SnBu_3$, $Pd(PPh_3)_4$, 15–73%.

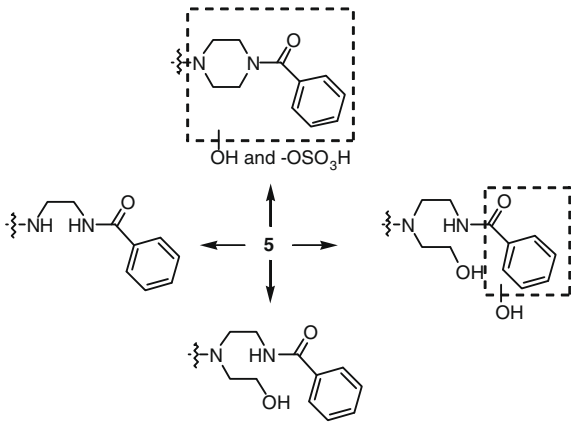

Figure 2. Metabolites of **5** identified in rat and human hepatocytes.

Table 2
Methylation of the piperazine ring

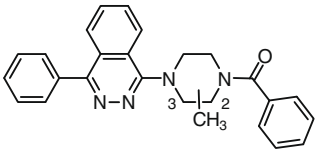

Compound	Piperazine	hSMO IC_{50}[a] (nM)	T.O. HLM[b] (%)	T.O. RLM[b] (%)	CYP 3A4 inhib.[c]	CYP 2D6 Inhib.[c]
5	Piperazine	19.0	19	12	<10	11
13	2-*S*-Me	5.3	<10	21	<10	11
14	2-*R*-Me	13.0	17	21	<10	<10
15	3-*S*-Me	11.0	<10	23	ND	ND
16	3-*R*-Me	2.2	44	39	<10	47

[a] Values are the mean of a minimum of two measurements with a standard deviation of 35% of the mean.
[b] Percent turnover after 30 min incubation with human (HLM) or rat (RLM) liver microsomes.
[c] Percent inhibition of CYP 3A4 or 2D6 at 3 μM concentration.

Table 3
Initial SAR around the pendant aryl group

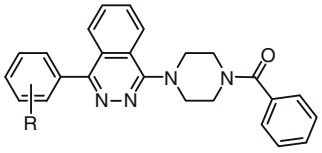

Compound	Phenyl	hSMO IC_{50}[a] (nM)	T.O. HLM[b] (%)	T.O. RLM[b] (%)	CYP 3A4 inhib.[c]	CYP 2D6 inhib.[c]
5	H	19.0	19	12	<10	11
17	3,4-Cl	17.3	31	10	<10	ND
18	4-Cl	5.2	20	10	16	24
19	4-CH_3	4.4	45	72	<10	<10
20	4-OCH_3	15.0	27	22	<10	19
21	4-F	10.8	17	10	<10	29
22	3-OCH_3	20.0	43	33	<10	19
23	3-CN	212.0	10	10	<10	18
24	2-CH_3	15.0	90	40	<10	24
25	2-Cl	20.3	62	15	<10	<10

[a] Values are the mean of a minimum of two measurements with a standard deviation of 35% of the mean.
[b] Percent turnover after 30 min incubation with human (HLM) or rat (RLM) liver microsomes.
[c] Percent inhibition of CYP 3A4 or 2D6 at 3 μM concentration.

Table 4
Aryl group substitutions within the 2-*S*-methyl piperazine series

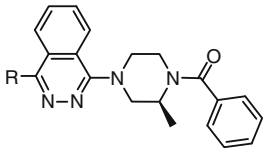

Compound	Aryl	hSMO IC_{50}[a] (nM)	T.O. HLM[b] (%)	T.O. RLM[b] (%)	CYP 3A4 inhib.[c]	CYP 2D6 inhib.[c]
13	Ph	5.3	10	21	<10	11
26	2-Pyridyl	110	<10	<10	<10	<10
27	3-Pyridyl	213	10	12	12	<10
28	4-Pyridyl	96	10	25	58	52
29	2-Pyridazyl	2340	<10	<10	<10	15
30	2-Oxazoyl	2700	10	23	<10	27
31	4-CH_3-Ph	3.2	38	43	13	10
32	4-Cl-Ph	7.0	<10	<10	40	43
33	4-F-Ph	11.8	10	15	20	18
34	4-CF_3-Ph	3.6	<10	<10	49	<10

[a] Values are the mean of a minimum of two measurements with a standard deviation of 35% of the mean.
[b] Percent turnover after 30 min incubation with human (HLM) or rat (RLM) liver microsomes.
[c] Percent inhibition of CYP 3A4 or 2D6 at 3 μM concentration.

Table 5
Effects of *p*-substituents on the phenyl ring in the 3-*R*-methyl piperazine series

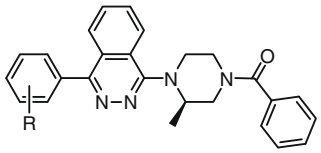

Compound	Phenyl	hSMO IC_{50}[a] (nM)	T.O. HLM[b] (%)	T.O. RLM[b] (%)	CYP 3A4 inhib.[c]	CYP 2D6 inhib. [c]
16	H	2.2	44	39	<10	<10
35	4-Cl	0.7	38	12	<10	60
36	4-CH_3	0.4	56	55	<10	<10
37	4-*c*Pr	2.3	34	21	31	<10
38	4-*i*Pr	7.3	41	73	14	20
39	4-*t*Bu	10.1	89	94	25	10
40	4-CH_2OH	2.7	14	13	15	<10
41	4-CN	3.1	<10	<10	12	<10
42	4-$N(CH_3)_2$	5.2	59	82	90	26
43	4-CF_3	2.8	13	11	<10	15

[a] Values are the mean of a minimum of two measurements with a standard deviation of 35% of the mean.
[b] Percent turnover after 30 min incubation with human (HLM) or rat (RLM) liver microsomes.
[c] Percent inhibition of CYP 3A4 or 2D6 at 3 μM concentration.

Table 6
In vivo pharmacokinetic properties of **43**

Species	Cl (IV, L/h/kg)	V_{dss}[c] (L/kg)	$t_{½}$[c] (h)	*F* (%)
Rat[a]	0.41	5.07	9.5	39
Mouse[b]	0.30	1.40	3.4	65
Dog[a]	0.20	2.96	10.0	60
Cyno[a]	0.53	2.52	4.3	31

[a] Nominal dose = 0.5 mg/kg iv, 2.0 mg/kg po.
[b] Nominal dose = 1.0 mg/kg iv, 2.0 mg/kg po.
[c] After iv dosing.

tolerance of *para*-substituents such as -Cl (**18**) and -F (**19**) was noted. Focusing then on the promise of the 2-*S*-methyl piperazine series, we explored modifications to the pendant aryl group in **13**.

As shown in Table 4, a number of aryl and heteroaryl groups were incorporated in compounds **26**–**34**. While heteroaryl replacements **26**–**30** were generally less potent, the previously noted tolerance of a *para*-substitution was confirmed in this series. Especially notable were 4-Cl and 4-CF_3 substituted compounds **32** and **34**, respectively, that afforded comparable potency without compromising stability in microsomes. Finally, we turned our attention to the 3-*R* methyl piperazine core to evaluate the effects of phenyl group substitution on stability within this more potent series. As illustrated in Table 5, introduction of a series of *para*-substituents onto the pendant phenyl ring in **16** afforded a number of promising compounds, including the sub-nanomolar hSMO antagonists **35** and **36**.

An excellent balance of properties was achieved with 4-CF_3 compound **43**. Compound **43** was potent in both our mSMO and hSMO assays with IC_{50}s of 2.0 and 2.8 nM, respectively. Moreover, an excellent cross-species in vivo pharmacokinetic profile of **43** was established in mouse, rat, dog, and cynomologous monkey (Table 6), enabling in vivo efficacy studies.

We sought to validate the in vivo Smo antagonism of **43** with a rodent hair follicle study. The role of the Shh pathway in hair follicle morphogenesis is well known, and the activation of the Shh signaling pathway in the skin of rodents following depilation has been used as a model of pathway antagonism with known Smo antagonists such as cyclopamine.[18] Adapted from the method of Paladini et al.,[19] the hind flanks of mice were depilated with wax to activate the hair follicle cycle. Five days after depilation, the mice were treated with a single oral dose[20] of 2, 20, or 100 mg/kg of compound **43**. After 6 h the skin was harvested and evaluated for induction of Gli1. A dose dependent reduction of Gli1 expression was observed reflecting an approximate EC_{50} = 2.0 μM, along

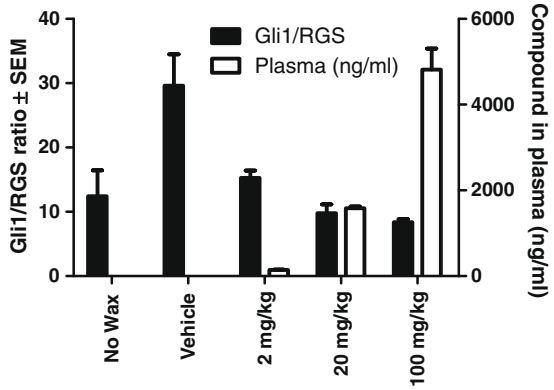

Figure 3. Reduction of Gli1 expression in skins of mice treated with **43**. Four mice per group, two samples per mouse: *r* (2 mg/kg) = 0.0016, *r* (20, 100 mg/kg) <0.0001 (Dunnett's method). For the no wax treatment, there were two mice per group, two samples per mouse. Gli1 RNA was measured using a quantitative real time PCR and was normalized to RGS (Pitx2) RNA.

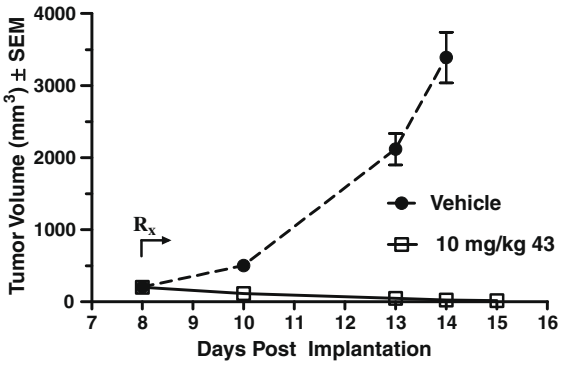

Figure 4. Tumor volume reduction in mouse Ptch +/− p53 −/− medulloblastoma model induced by treatment with 10 mg/kg **43**, QD oral. Ten mice per group, $\rho < 0.0001$ (Dunnett's method).

with a corresponding dose-dependant increase in plasma exposure of **43** (Fig. 3).

Having established the in vivo modulation of Smo signaling in the rodent hair follicle model, we sought to evaluate the efficacy of compound **43** in a rodent tumor model. It has been well established that Ptch +/− mice are prone to develop medulloblastomas. Addition of a second genetic defect such as p53 −/− increases the incidence and decreases the latency associated with development of these tumors.[21] Following the method of Sasai et al.,[22] p53 −/− and Ptch +/− mice were crossbred. Tumors from p53 −/− Ptch +/− mice were harvested and transplanted into immunocompromised mice. After 8 days, the tumor-allograft bearing mice were randomized and separated into a treatment group (10 mg/kg **43** QD, oral)[20] and control group (vehicle). As shown in Figure 4, the treatment group showed inhibition of tumor growth relative to control, and significant tumor volume reduction on day 15 with respect to onset of treatment on day 8.

In conclusion, we have described the evolution of a class of 4-aryl-1-piperazinyl phthalazines as potent and metabolically stable antagonists of SMO. Replacement of the thiophene ring in **1** with a phenyl group significantly improved the outcome in our rat and human microsomal stability assays. The interplay of piperazine methylation and aryl group substitution was explored, elucidating the SAR of concomitant changes to these regions. Ultimately the in vivo efficacy of **43** was demonstrated in a Ptch +/− medulloblastoma tumor allograft model.

References and notes

1. Ingham, P. W.; McMahon, A. P. *Genes Dev.* **2001**, *15*, 3059.
2. Rubin, L. L.; de Sauvage, F. J. *Nat. Rev. Drug Disc.* **2006**, *5*, 1026.
3. Lum, L.; Beachy, P. A. *Science* **2004**, *304*, 1755.
4. Epstein, E. H. *Nat. Rev. Cancer* **2008**, *8*, 743.
5. Berman, D. M.; Karhadkar, S. S.; Hallahan, A. R.; Pritchard, J. I.; Eberhart, C. G.; Watkins, D. N.; Chen, J. K.; Cooper, M. K.; Taipale, J.; Olson, J. M.; Beachy, P. A. *Science* **2002**, *297*, 1559.
6. (a) Taipale, J.; Chen, J. K.; Cooper, M. K.; Wang, B.; Mann, R. K.; Milenkovic, L.; Scott, M. P.; Beachy, P. A. *Nature* **2000**, *406*, 1005; (b.) Incardona, J. P.; Gaffield, W.; Kapur, R. P.; Roelink, H. *Development* **1998**, *125*, 3553; (c) Cooper, M. K.; Porter, J. A.; Young, K. E.; Beachy, P. A. *Science* **1998**, *280*, 5369.
7. (a) Miller-Moslin, K.; Peukert, S.; Jain, R. K.; McEwan, M. A.; Karki, R.; Llamas, L.; Yusuff, N.; He, F.; Li, Y.; Sun, Y.; Dai, M.; Perez, L.; Michael, W.; Sheng, T.; Lei, H.; Zhang, R.; Williams, J.; Bourret, A.; Ramamurthy, A.; Yuan, J.; Guo, R.; Matsumoto, M.; Vattay, A.; Maniara, W.; Amaral, A.; Dorsch, M.; Kelleher, J. F. *J. Med. Chem.* **2009**, *52*, 3954; Review of recent efforts in the field of Hh signaling regulation: (b) Mahindroo, N.; Punchihewa, C.; Fujii, N. *J. Med. Chem.* **2009**, *52*, 3829; (c) Peukert, S.; Jain, R. K.; Geisser, A.; Sun, Y.; Zhang, R.; Bourret, A.; Carlson, A.; DaSilva, J.; Ramamurthy, A.; Kelleher, J. F. *Bioorg. Med. Chem. Lett.* **2009**, *19*, 328; (d) Tremblay, M. R.; Nevalainen, M.; Nair, S. J.; Porter, J. R.; Castro, A. C.; Behnke, M. L.; Yu, L.-C.; Hagel, M.; White, K.; Faia, K.; Grenier, L.; Campbell, M. J.; Cushing, J.; Woodward, C. N.; Hoyt, J.; Foley, M. A.; Read, M. A.; Sydor, J.; Tong, J. K.; Palombella, V. J.; McGovern, K.; Adams, J. *J. Med. Chem.* **2008**, *51*, 6646; (e) Feldmann, G.; Fendrich, V.; McGovern, K.; Bedja, D.; Bisht, S.; Alvarez, H.; Koorstra, J.-B. M.; Habbe, N.; Karikari, C.; Mullendore, M.; Gabrielson, K. L.; Sharma, R. *Mol. Cancer Ther.* **2008**, *7*, 2725; (f) Brunton, S. A.; Stibbard, J. H. A.; Rubin, L. L.; Kruse, L. I.; Guichert, O. M.; Boyd, E. A.; Price, S. *J. Med. Chem.* **2008**, *51*, 1108; (g) Remsberg, J. R.; Lou, H.; Tarasov, S. G.; Dean, M.; Tarasova, N. I. *J. Med. Chem.* **2007**, *50*, 4534; (h) Dessole, G.; Branca, D.; Ferrigno, F.; Kinzel, O.; Muraglia, E.; Palumbi, M. C.; Rowley, M.; Serafini, S.; Steinkühler, C.; Jones, P. *Bioorg. Med. Chem. Lett.* **2009**, *19*, 4191; (i) Tremblay, M. R.; Lescarbeau, A.; Grogan, M. J.; Tan, E.; Lin, G.; Austad, B. C.; Yu, L. C.; Behnke, M. L.; Nair, S. J.; Hagel, M.; White, K.; Conley, J.; Manna, J. D.; Alvarez-Diez, T.; Hoyt, J.; Woodward, C. N.; Sydor, J. R.; Pink, M.; MacDougall, J.; Campbell, M. J.; Cushing, J.; Ferguson, J.; Curtis, M. S.; McGovern, K.; Read, M. A.; Palombella, V. J.; Adams, J.; Castro, A. C. *J. Med. Chem.* **2009**, *52*, 4400.
8. (a) Austin, R. J.; Kaizerman, J.; Lucas, B.; McMinn, D. L.; Powers, J. PCT Int. Appl. WO 2009/002469 A1, 2009; (b) Kaizerman, J.; Lucas, B.; McMinn, D. L.; Zamboni, R. PCT Int. Appl. WO 2009/035568 A1, 2009.
9. *IC_{50} assay for mouse Smo:* The mouse Smoothened activity was measured in vitro using a modified version of the method described by Chen et al. (Chen, J. K; Taipale, J.; Young, K. E.; Maiti, T.; Beachy, P.A. *Proc. Natl. Acad. Sci. U.S.A.* **2002**, 14071). An oligonucleotide cassette with five consensus Gli1 binding sites was ligated into the luciferase reporter plasmid pGL4.16 (Promega, Madison, WI, USA). A stable clone of NIH-3T3 cells stably transfected with the Gli1-binding-site plasmid was used for the reporter assay. To measure compound activity, compounds were incubated with cells for 15 h in the presence of Optimem medium (Invitrogen, Carlsbad, CA, USA) supplemented with 0.5% charcoal–dextran treated fetal bovine serum (HyClone) and 10 mM myristoylated mouse Shh protein (Williams et al., 1999). Luciferase activity was measure by addition of Bright-Glo (Promega) and reading on a luminometer. For a single IC_{50} assay, compounds were tested in quadruplicate using a threefold dilution series. Assays were performed in 384-well plates.
10. *IC_{50} assay for human Smo:* HEPM cells were used to measure human Smo activity in vitro using a modified version of the method described in US Patent 6,613,798. In 96-well tissue culture plates compounds were incubated with HEPM cells in the presence of MEM media supplemented with 0.5% charcoal–dextran treated fetal bovine serum (HyClone) and 50 mM myristoylated mouse Shh protein. (Williams, K. P.; Rayhorn, P.; Chi-Rosso, G. Garber, E. A.; Strauch, K. L.; Horan, G. S. B.; Reilly, J. O.; Baker, D. P.; Taylor, F. R.; Koteliansky V.; Pepinsky, R. B. *J. Cell Sci.* **1999**, *112*, 4405.) Twenty-four hours after the addition of compound and Shh, GLI expression was measured using a Quantigene assay (Affymetrix, Santa Clara, CA, USA).
11. Pooled human or rat liver microsomes (0.25 mg/mL) were incubated at 37 °C in a phosphate buffer (pH 7.4) with the test compound (1 μM). The reaction was started with the addition of NADPH (1 mM final concentration). Incubations were stopped after 0 or 30 min with the addition of organic solvent. Quenched samples were analyzed for unchanged test compound by reversed phase HPLC with tandem mass spectrometric detection. Percent turnover is determined by the ratio of the amount (peak area) of unchanged test compound remaining in incubated samples to the amount of unchanged test compound in non-incubated samples (0 min).
12. *CYP 3A:* Pooled human liver microsomes (0.1 mg/mL) were incubated at 37 °C in a phosphate buffer (pH 7.4) with the selective 3A substrate midazolam at a concentration of 2.5 μM in the presence and absence of test compound (3 μM). The reaction was started with the addition of NADPH (1 mM final concentration). Incubations were stopped after 5 min with the addition of organic solvent and 1-hydroxymidazolam metabolite formation is measured by an HPLC–MS detection method. Inhibition was determined by the ratio of the amount of metabolite in the presence of test compound to the amount of metabolite in the absence of test compound. *CYP 2D6:* Pooled human liver microsomes (0.25 mg/mL) were incubated at 37 °C in a phosphate buffer (pH 7.4) with the selective 2D6 substrate bufuralol at a concentration of 5 μM in the presence and absence of test compound (3 μM). The reaction was started with the addition of NADPH (1 mM final concentration). Incubations were stopped after 10 min with the addition of organic solvent and 1-hydroxybufuralol metabolite formation was measured by an HPLC/MS detection method. Inhibition is determined by the ratio of the amount of metabolite in the presence of test compound to the amount of metabolite in the absence of test compound.
13. Purity of all final compounds was assessed by HPLC and determined to be >95%. The structures were confirmed by ^{1}H NMR and LC/MS. The enantiomeric purity of chiral compounds was >98% and as determined by chiral HPLC in comparison to a racemic reference standard.
14. Chekmarev, D. S.; Stepanov, A. E.; Kasatkin, A. N. *Tetrahedron Lett.* **2005**, *46*, 1303.
15. Castro, M. E.; Rosa, E.; Osuna, J. A.; Garcia-Ferraro, T.; Loza, M.; Cadavid, M. I.; Fontenla, J. A.; Masaguer, C. F.; Cid, J.; Raviña, E.; García-Mera, G.; Rodriguex, J.; de Ceballos, M. L. E. *Eur. J. Med. Chem.* **1994**, *29*, 831.
16. Cryopreserved human or rat hepatocytes (1 million/mL, Celsis) were incubated at 37 °C and 5% CO_2 controlled environment with the test compound (10 μM) in a commercially available hepatocytes incubation buffer (Celsis). The reaction was stopped after 2 h with the addition of organic solvent. Quenched samples were analyzed by reversed phase HPLC coupled with tandem mass spectrometry detection. Metabolites are identified using various mass spectrometry scans, for example, precursor ion scan, product ion scan, and multiple-reaction monitoring. Metabolites of the test compounds generated in the given condition were proposed based on their molecular ion mass and mass fragmentation pattern observed in mass spectrometry.
17. Topliss, J. G. *J. Med. Chem.* **1977**, *20*, 463.
18. Chiang, C.; Swan, R. Z.; Grachtchouk, M.; Bolinger, M.; Litingtung, Y.; Robertson, E. K.; Cooper, M. K.; Gaffield, W.; Westphal, H.; Beachy, P. A.; Dlugosz, A. A. *Dev. Biol.* **1999**, *205*, 1.
19. (a) Paladini, R. D.; Saleh, J.; Qian, C.; Xu, G.-X.; Rubin, L. L. *J. Invest. Dermatol.* **2005**, *125*, 638; (b) Faia, K. L.; Mandley, E.; Niu, Q.; Pien, C.S. PCT Int. WO2008/089123 A2.
20. In 25% 2-hydroxypropyl-beta-cyclodextrin in water, 10 mL/kg.
21. Wetmore, C.; Eberhart, D. E.; Curran, T. *Cancer Res.* **2001**, *61*, 513.
22. Sasai, K.; Romer, J. T.; Lee, Y.; Finkelstein, D.; Fuller, C.; McKinnon, P. J.; Curran, T. *Cancer Res.* **2006**, *66*, 4215.